

# At-Speed Defect Localization by Combining Laser Scanning Microscopy and Power Spectrum Analysis

Mary A. Miller, Edward I. Cole, Jr.,  
Garth M. Kraus and Perry J. Robertson  
Sandia National Laboratories  
Albuquerque, NM 87185  
505-845-5883

## *Invited Paper*

**Abstract**—The defect detection capabilities of Power Spectrum Analysis (PSA) [1] have been successfully combined with local laser heating to isolate defective circuitry in a high-speed Si Phase Locked Loop (PLL). The defective operation resulted in missed counts when operating at multi-GHz speeds and elevated temperatures. By monitoring PSA signals at a specific frequency through zero-spanning and scanning the suspect device with a heating laser (1340 nm wavelength), the area(s) causing failure were localized. PSA circumvents the need for a rapid pass/fail detector like that used for Soft Defect Localization (SDL) [2] or Laser-Assisted Defect Analysis (LADA) [3] and converts the at-speed failure to a DC signature. The experimental setup for image acquisition and examples demonstrating utility are described.

**Index Terms**—Si PLL, PSA, SDL, LADA, missing count, functional failure

## I. INTRODUCTION

Defect localization in high-speed devices can be complicated when requiring operation at GHz frequencies to exercise a defect. Thermally sensitive defects have been successfully localized using Soft Defect Localization (SDL) [2] or its photocurrent leakage counterpart Laser-Assisted Defect Analysis (LADA) [3], but detection of the failing condition during at-speed operation can be difficult. A more generally applicable and direct detection method for high-frequency failing conditions is of value in the failure analysis process.

The need for such a detection scheme was encountered when performing failure analysis of a high-speed Si Phase Locked Loop (PLL) that showed defective operation at elevated temperatures. The failure resulted in an intermittent missed count within a high-speed counter sub-circuit. Utilizing typical failure analysis techniques such as LIVA[4] and TIVA[5], the digital counter and voltage regulator regions were identified. However, isolation of a particular failure cause was not evident.

Traditional SDL/LADA [3] was not attempted since the failure was not necessarily a conventional pass/fail and presented as an intermittent clock change. A technique was needed to both monitor the frequency portion of the failure and to feedback that information for localization.

An existing technique that is very sensitive to the frequency component of devices is Power Spectrum Analysis (PSA) [1][6]. In PSA, a spectrum analyzer is connected to the device pins and the dynamic frequency-domain response under stimulus is recorded. An example PSA setup includes a square wave input on the device power pin with a magnitude less than or equal to the operating voltage. Depending on the loading and dynamic impedance of the device, the square wave is modulated. Distinctive device signatures are then obtained under those operating conditions. The technique can collect a tremendous amount of data over the frequency range selected. A comparison of the collected spectra to a control or standard spectra highlights differences between devices. Subtle changes between parts or in the loading of parts may translate to a single peak or trending in peaks within a frequency range. However, identifying and simulating how certain faults or electrical characteristics change the spectrum is a challenging effort.

To address the failure analysis needs presented by the Si PLL, a combination of thermal stimulus (global and a scanned laser) and the detection sensitivity of PSA was developed. PSA was used to characterize the frequency dependence of the failure and obtain the spectral differences in a passing and failing condition. Once identified, the difference peaks that appear in the spectrum are zero-spanned and their amplitude used to modulate the image contrast as a function of either thermal or photocurrent laser positions. Regions and circuitry can be localized to describe the defective behavior of failing devices. While global heating is used to generate initial zero-spanned

frequencies ( $F_0$ ), local heating is subsequently used to determine zero-spanned frequencies ( $F_1$  and  $F_2$ ) for effective circuitry localization. Through PSA spectrum comparisons and subsequent zero-spanned imaging, a big data problem is effectively filtered to produce a DC-image of an at-speed operating failure.

The experimental approach, equipment set-up, and examples of zero-spanned images are included below along with a discussion of the indicated failure properties.

## II. FAILURE DESCRIPTION AND EXPERIMENTAL APPROACH

Localizing the area(s) responsible for introducing failures on a Si PLL was the primary focus for methodology development. Several of the high-speed counters failed at elevated temperatures with normal biasing. While the temperature was elevated, the failing conditions were within the specifications for operation. The failure manifested itself as intermittently reporting an erroneous count value. Multiple devices displayed similar failing signatures. The temperature of the test board and Si device was selected using a temperature chuck on a digitally controlled hotplate.

The PSA setup used to acquire spectra has been described in previous publications [1][6]. The major components are the spectrum analyzer, a means of providing dynamic stimulus to the device being tested and fixturing/cabling for the sample. The dynamic stimulus in PSA can be made by varying the power supply voltage (such as a square applied to  $V_{DD}$ ) or by dynamic device operation. A power spectrum is collected under dynamic stimulus. An example spectrum is shown in Fig. 1; there is a large amount of information contained in the PSA spectrum. The specifics of the data and spectral shape depend on the spectrum analyzer settings (bandwidth, frequency span, averaging, etc.), the dynamic stimulus applied, and the fixture/target sample. One distinction from PSA as described elsewhere [1][6], is that periodic waveforms are inputs into the power or input pin. Here, the PSA spectra are monitoring the functionality of the device with no extra injection of periodic waveform.

In practice PSA compares the collected spectrum with a reference. This comparison (usually done by dividing the two spectra to yield a normalized result) can produce a much simpler data set for difference visualization. An example of a normalized spectra with reduced information is shown in Fig. 2. By zero-spanning, the power at a specific frequency can be collected. The advantage in zero-spanning is that changes in power at the selected frequency can be updated quickly. This feature is necessary to produce images in a reasonable time frame (1-2 minutes).

The spectrum analyzer used for our analysis, an Agilent N9010A, has an analog output for the spectral power when using zero-spanning. This made for an easily integrated signal to produce image contrast.

Difference spectra on the Si PLL counter identified frequencies where the power spectrum changed between passing and failing temperatures. These were the frequencies selected for zero-spanning.

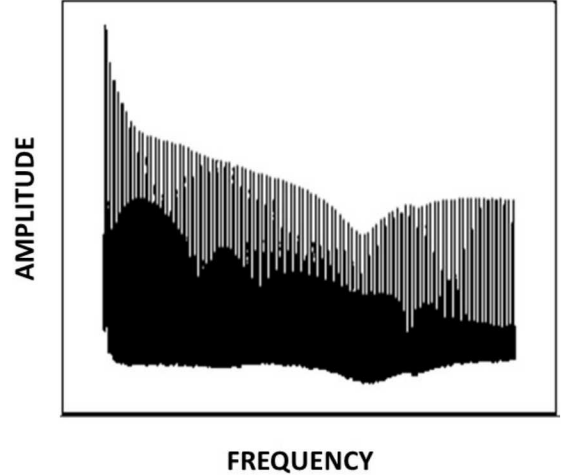


Figure 1. Example spectrum collected using the PSA system.

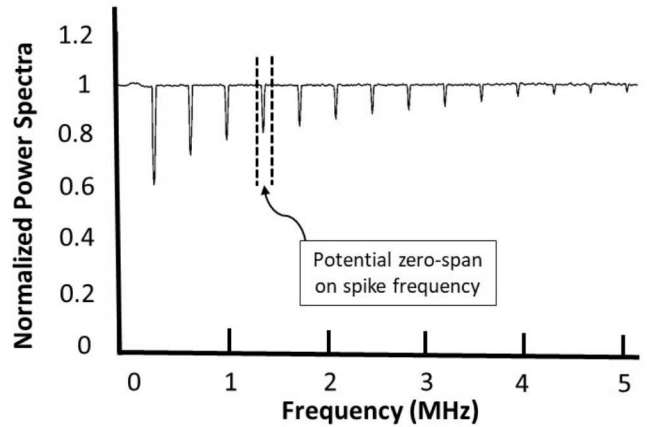


Figure 2. Normalized PSA spectrum example showing differences between device conditions. Zero-spanning on a given frequency will yield the power information at the selected frequency only.

To generate an image of where local heating produced a failing condition, the Si device, the test system biasing the sample, the global thermal control system, the PSA spectrum analyzer and a scanning laser microscope system were integrated (Fig. 3). The temperature chuck was controlled to bring the Si device just below the temperature at which failures are detected. The scanned lasers were then used to produce failures by additional heating or photocurrent loading. In concept this is similar to the effects used in SDL and LADA, but with image contrast determined by the power at the zero-spanning frequency as opposed to a pass/fail condition.

Once the initial images were collected, they were used to further refine the frequency for zero-spanning. This process is described in the Experimental Results section below.

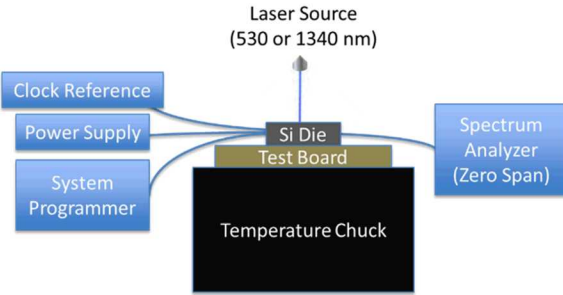


Figure 3. Combined PSA, global heating and laser setup.

### III. EXPERIMENTAL RESULTS

Initially the failing Si device was analyzed using TIVA and LIVA. These techniques were not capable of narrowing down the search space to a single localized failure. Given the functional nature of the failure, SDL was considered. The failure occurred intermittently at temperature and speed. Instrumenting a simple pass/fail condition at frequency would be a significant challenge. Previous work with PSA had proven a powerful technique to monitor subtle dynamic loading differences between microcontrollers with different date codes, memory sizes, or even aged devices[1]. To leverage the PSA sensitivity, a set-up was assembled as described above.

As a first step, the power spectra were taken of the device in both the at-speed passing and failing conditions. This was done by globally increasing the temperature of the device to  $44.8^{\circ}\text{C}$  using the temperature-controlled hotplate. Under these conditions, the counter begins to start missing counts at speed. There were differences in the spectra: peaks that were present in one condition were missing in the other. As the failing counter was sensitive to temperature, we wanted to take advantage of the SDL-like behavior and heat the sample to the temperatures just below the onset of failure before scanning with the thermal laser.

Using a difference pass/fail frequency peak ( $F_0$ ) identified by PSA, image contrast was based on the power amplitude at  $F_0$ . The spectrum analyzer was set to zero-span at  $F_0$  while the laser scanned over the device. Signal amplification and averaging similar to standard TIVA and LIVA were used to improve the signal-to-noise ratio (SNR). In the resulting zero-span images at  $F_0$ , dark signals indicate regions where the 1340 nm laser reduced the amplitude of the zero-spanned peak, while bright signals indicate regions where the thermal laser increased the amplitude of the  $F_0$  peak (passing condition). The inference is that dark regions are circuitry that begin to make the counter fail when heated—a simulation of the failure conditions.

An amplitude map of  $F_0$  is shown in Fig. 4. The image is a zero-spanned frequency map or power amplitude map based on PSA spectra. We will refer to these as  $F_0$  *amplitude maps*. The amplitude map in Fig. 4 indicates three contrast regions. The top

right corner of the amplitude map indicates the digital voltage regulator. The region on the left of the image is the analog voltage regulator. These were not considered areas of interest as small voltage circuit imbalances near failure conditions are expected to produce failures. Further analysis of these regions was not pursued. The other interesting feature in the image is the pre-scaler circuitry of a high-speed digital counter, which is also shown at higher magnification in Fig. 5.

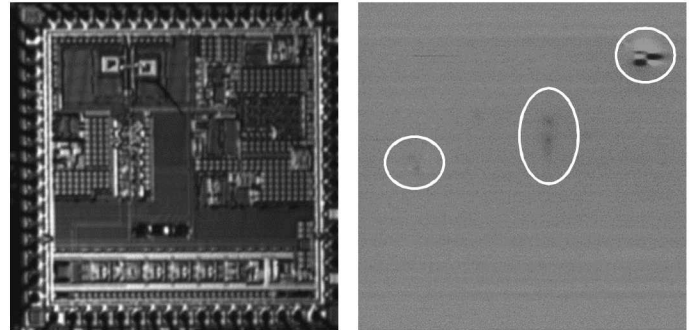


Figure 4. 1340 nm Reflected light image (left) and representative amplitude map for  $F_0$  (right) at  $44.8^{\circ}\text{C}$ .

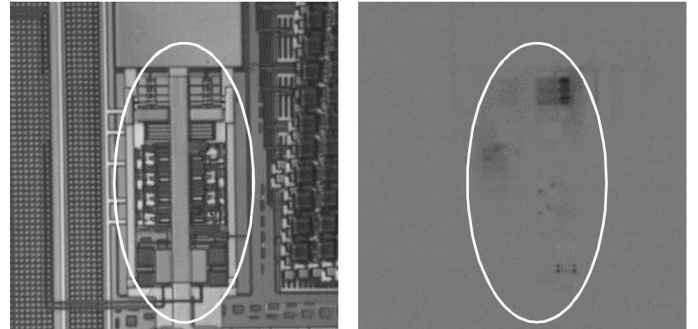


Figure 5. 1340 nm Reflected light image (left) and amplitude map taken of the pre-scaler at  $F_0$ .

The two vertical parallel structures in Fig. 5 should be operating as a matched pair. There is an asymmetry in the signal caused by an imbalance on the circuit output loading. Further localization was difficult because within this circuit there were still multiple areas producing dark  $F_0$  signals. It was also unclear whether these signals were symptoms or the cause of failure.

Similar to the thermal laser stimulus, an  $F_0$  *amplitude* image was collected using a 532 nm, photocurrent-producing laser. The resultant reflected light image and frequency map are shown in Fig. 6. The pre-scaler circuitry no longer shows up, but the analog and digital voltage regulators do.

Higher magnification images of the analog regulator also show the varactor, part of the Voltage Controlled Oscillator (VCO). The image in Fig. 7 is dominated by photocurrent effects; however, the diffuse dark signal in the white box may be due to slight heating by the green laser. Voltage shifts in the

varactor circuit directly modulate the output frequency, which could be induced by either photocurrent or temperature. The asymmetry is consistent with the failure mode, but this site is not thought to be the cause of failure.

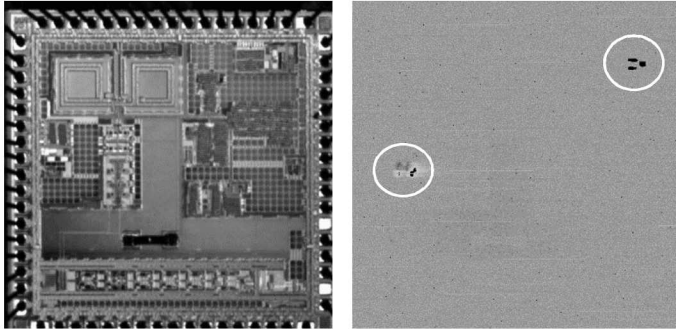


Figure 6. 532 nm Reflected light image (left) and representative amplitude map at  $F_0$  (right) at  $44.8^\circ\text{C}$

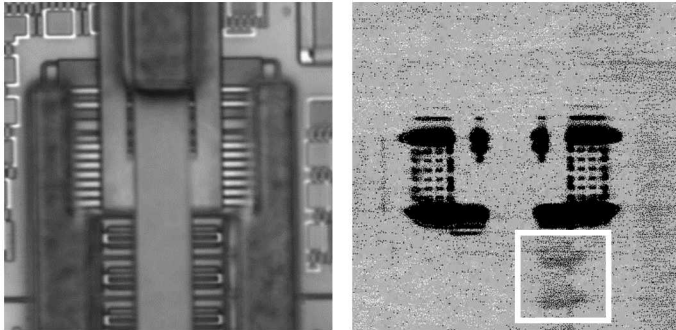


Figure 7. 532 nm Reflected light image (left) and representative amplitude map at  $F_0$  (right) of the varactor circuit.

The initial passing and failing power spectrums, and thus the discriminating amplitude map  $F_0$ , were based on a global temperature condition, i.e. the entire device was placed on a hot plate to simulate failure. To further discriminate symptoms from cause, the next amplitude maps were generated by comparing the passing and failing power spectra under local heating. The Si PLL counter temperature was held just below the passing/failing threshold. Power spectra were collected with the thermal laser spotted on dark regions identified in the  $F_0$  amplitude map in Fig. 5 (failing conditions) and compared to background and bright regions (passing conditions). The goal was to identify the local thermal effects vs the global ones, assuming they would better isolate the failure. A new failing spectrum was generated with peaks and valleys that appeared and disappeared based on the position of the thermal laser. By zero-spanning on one of the newly identified frequencies ( $F_1$ ) that did not appear in the global heating spectra, additional amplitude maps were acquired based on local heating.

The  $F_1$  amplitude maps identified a divide-by-2 of the counter sub-circuitry as a potential failure source (Fig. 8). For purposes of resolution, the site was further imaged with

photocurrent zero-span amplitude maps. These images are shown in Fig. 9.

The new maps (Fig. 9) indicated different regions of interest than the  $F_0$  amplitude maps. By repeating the methodology used to select  $F_1$ , a new zero-spanned frequency,  $F_2$ , was selected from the  $F_1$  frequency maps. The  $F_2$  frequency map, shown in Fig. 10, also indicates the divide-by-2 counter.

A very strong signal (arrow) showed up in the Fig. 10 map. When spotting the thermal laser on this strong signal area, the counter could be made to fail with lower thermal chuck heating. Other sites would modulate the amplitude of  $F_2$ , but this site was the one that caused failure. Other  $F_2$  frequencies based on  $F_1$  images, indicated the same divide-by-2 circuitry.

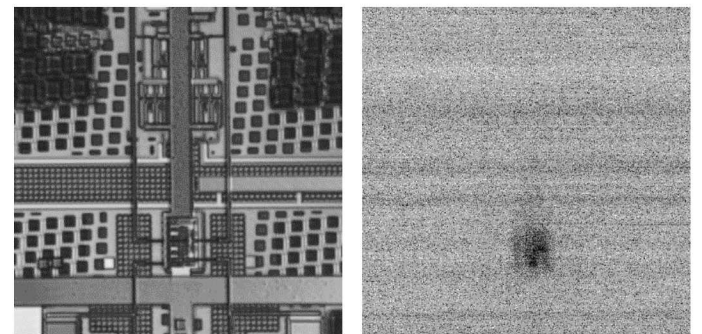


Figure 8. 1340 nm Reflective Light image and corresponding amplitude map at  $F_1$  highlighting a divide-by-2 counter.

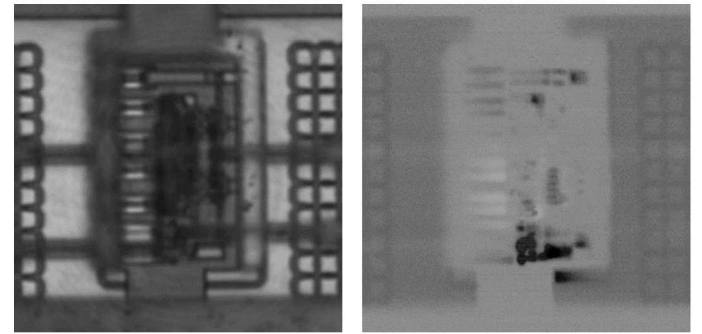
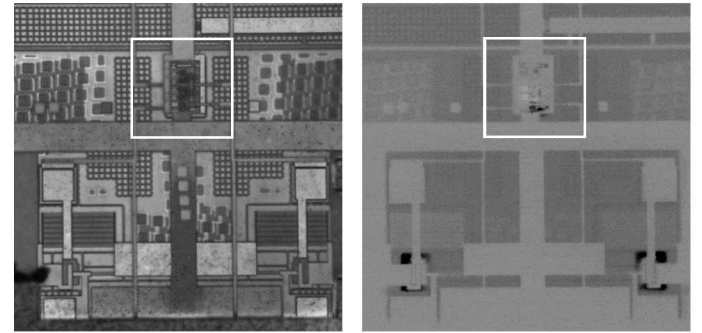


Figure 9. Top images: 532 nm Reflected Light Image and corresponding  $F_1$  amplitude map of the analog amp and divide-by-2 circuitry

(white box). The bottom images are a higher magnification image of the divide-by-2 circuitry.

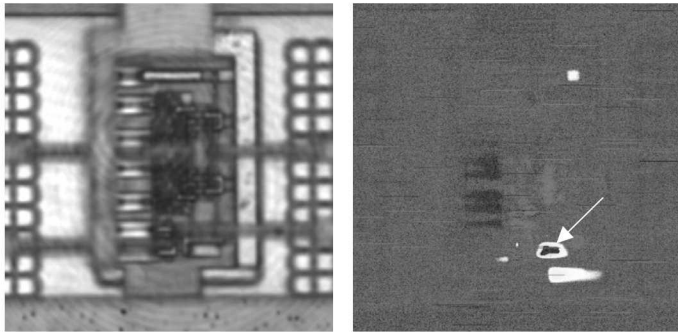


Figure 10. 532 nm Reflected Light Image and corresponding F2 amplitude map. The arrow indicates the most thermally sensitive area in the divide-by-2 circuitry.

Using the iterative process with multiple frequencies the failure was localized to the divide-by-2 circuitry shown in Figs. 8, 9 and 10. In addition, this failure was validated in circuit simulation. The asymmetry initially thought to be caused by an input imbalance on the circuit, was later found to be an imbalance on the loading of the circuit outputs. Further failure analysis on the parts was not pursued as this localization satisfied the needs of the customer.

#### IV. SUMMARY AND CONCLUSIONS

We have described a method for localizing at-speed failures on high-frequency devices. The method is based on a combination of localized thermal stimulus and PSA. We leveraged the frequency-detection sensitivity of PSA and the ability to zero-span on a specific frequency of interest to generate frequency-specific amplitude maps. The contrast in these amplitude maps indicate localized passing and failing conditions. The first frequency-specific amplitude maps were primarily driven by global heating and indicated areas for subsequent local laser heating and new frequency selection. Iteratively selecting new zero-span frequencies facilitated defective circuit localization. This combined methodology filtered a big data problem into a single frequency, effectively converting a high-speed failure into a DC signature.

#### ACKNOWLEDGMENT

The authors gratefully acknowledge the contributions of Paiboon Tangyunyong for PSA consultation.

Sandia National Laboratories is a multimission laboratory managed and operated by National Technology & Engineering Solutions of Sandia, LLC, a wholly owned subsidiary of Honeywell International Inc., for the U.S. Department of Energy's National Nuclear Security Administration under contract DE-NA0003525.

This paper describes objective technical results and analysis. Any subjective views or opinions that might be expressed in the

paper do not necessarily represent the views of the U.S. Department of Energy or the United States Government.

#### REFERENCES

- [1] P. Tangyunyong, E.I. Cole, Jr., G.M. Loubriel, J. Beutler, D.M. Udoni, B.S. Paskaleva, and T.E. Buchheit, "Power Spectrum Analysis (PSA)," in *Proc. From the 43<sup>rd</sup> International Symposium for Testing and Failure Analysis*, 2017, pp. 73-78.
- [2] M. R. Bruce, V. J. Bruce, D. H. Eppes, J. Wilcox, E. I. Cole, P. Tangyunyong, and C. F. Hawkins, "Soft Defect Localization (SDL) on ICs," *Proceedings of 28<sup>th</sup> International Symposium for Testing and Failure Analysis*, Phoenix, Arizona, November 2002, pp. 21-27.
- [3] J.A. Rowlette and T.M. Eiles, "Critical Timing Analysis in Microprocessors Using Near-IR Laser Assisted Device Alteration (LADA)," *ITC International Test Conference*, 2003, pp. 264 – 273.
- [4] E. I. Cole, Jr., J. M. Soden, J. L. Rife, D. L. Barton, and C. L. Henderson, "Novel failure analysis techniques using *photon probing* with a scanning optical microscope", in the *International Reliability Physics Symposium* (1994), p. 388.
- [5] E. I Cole, Jr., P. Tangyunyong, D. A. Benson, and D. L. Barton, "TIVA and SEI Developments for Enhanced Front and Backside Interconnection Failure Analysis," *Microelectronics Reliability* 39 (1999), 991.
- [6] P. Tangyunyong, E.I. Cole, Jr., G.M. Loubriel, and J. Beutler, "Scanning Method for Screening of Electronic Devices," U.S. Patent 10,094,874, Oct. 9, 2018.